Joint Special Interest Group meeting between euspen and ASPE
Advancing Precision in Additive Manufacturing
Inspire AG, St. Gallen, Switzerland 2021
www.euspen.eu

Characterizing shrinkage and quality of ceramic two-photon printed microstructures

John Cortes[1], Magi Mettry[1], Matthew Worthington[1], Swetha Chandrasekaran[1], Robert Panas[1]

[1]Lawrence Livermore National Laboratory, Livermore, CA, USA

Corresponding author: JohnCortes@llnl.gov

Abstract

Characterizing the optimal printing parameters and shrinkage of polymer-derived ceramic (PDC) resins is important to integrate these promising materials into future MEMS/NEMS applications. These ceramic materials offer better mechanical and thermal properties for devices which are designed to operate in extreme or highly dynamic environments. This work studies and characterizes the optimal 2-photon polymerization printing parameters for SiOC ceramic resins. The study found that these resins print optimally the Nanoscribe laser power settings are within the 35%-45% range and the scan speed are within 6,000 µm/s to 8,000 µm/s. In addition, the qualitative properties of the prints were also studied through SEM imaging. Defects and distortion as a function of laser power and laser scan speed were also characterized. Additionally, the shrinkage of the PDC material was characterized as a function of scan passes (which affects proportion of fully cross-linked volume) before and after the pyrolysis process. This study found that doing up to three passes per voxel can reduce overall linear shrinkage from about 47% to 35%. Lastly, a proposed method of dealing with this shrinkage in functional structures is proposed. Strain relief structures are introduced with the goal of maintaining the structure/s center line aligned during shrinkage. This will be valuable for devices which will require alignment and transfer onto a separate substrate.

Key words: ceramic, microstructures, two-photon printing, shrinkage

1. Introduction

The last ten to fifteen years has brought upon a revolution in prototyping and rapid product development led by advances in additive manufacturing (AM) technologies. Additive manufacturing creates the opportunity to manufacture highly intricate 3D structures using a single, highly repetitive process one layer at a time. Although most of that work has focused on macro-scale printing processes with plastics (and more recently, metals and composites), a significant scientific push has been made to also develop micro-scale processes [1, 2, 3]. Two-photon Polymerization (2PP) is one of the technologies that has allowed for development of 3D printed microstructures. 2PP utilizes femtosecond laser pulses with two-photon absorption to generate features using a wide variety of photon-activated photoresists and resins with a resolution as high as 100 nm [4]. The print resolution of 2PP processes is determined by the exposure dose to the smallest polymerized volume. This dose is determined both by the pulse energy and the scanning speed [5].

Most of these resins result in polymer structures which are limited in their application due to their poor mechanical properties. However, the use of ceramic resins has recently been developed for 2PP processes [6, 7]. They generally come in the form of polymer-derived ceramics (PDC) and are highly tuneable based on their molecular compositions. While these resins feature much more favourable mechanical properties, they tend to shrink anywhere from 30-55% during post-processing [8, 9]. This may not be desirable and difficult to design for in precise MEMS/NEMS applications, therefore it is crucial that this shrinkage be fully understood and characterized. In this work, we study the shrinkage of 2PP-printed silicon oxycarbide (SiOC) microstructures with a 100:1 aspect ratio. Additionally, we study ways to reduce this shrinkage in self-centering disk structures. 3D printed ceramic flexures at the microscale would be useful in MEMS devices that require complex geometries with low thermal conductivities.

2. Methods

The microscale two-photon printing process was performed using a NanoScribe GmbH Photonic Professional GT system at LLNL's Advanced Manufacturing Laboratory (AML) facility. This system features a 150mW (at 100% power) femtosecond laser source with a center wavelength of 780 nm and a pulse width of ~100 fs. A 63x 1.4 NA oil immersion lens (Carl Zeiss) was used for optimal print resolution. A single-side polished silicon chip measuring approximately 1" by 1" was coated with 3-(Trimethoxysilyl)propyl methacrylate (Silane) for 5 minutes at a temperature of 90 °C to enhance surface adhesion. A small drop of the custom polymer-derived ceramic (PDC) resin was applied to the polished side of the silane-treated silicon chip. The structures were printed up-side-down using the "dip-in laser lithography" method. The prints were then developed by submerging them in propylene glycol monomethyl ether acetate (PGMEA) for four hours. This process removes any unpolymerized solution

After full development in the PGMEA solution, the sample was dried using an EMS 3100 critical point drying system. After critical-point-drying, the samples were pyrolyzed in a

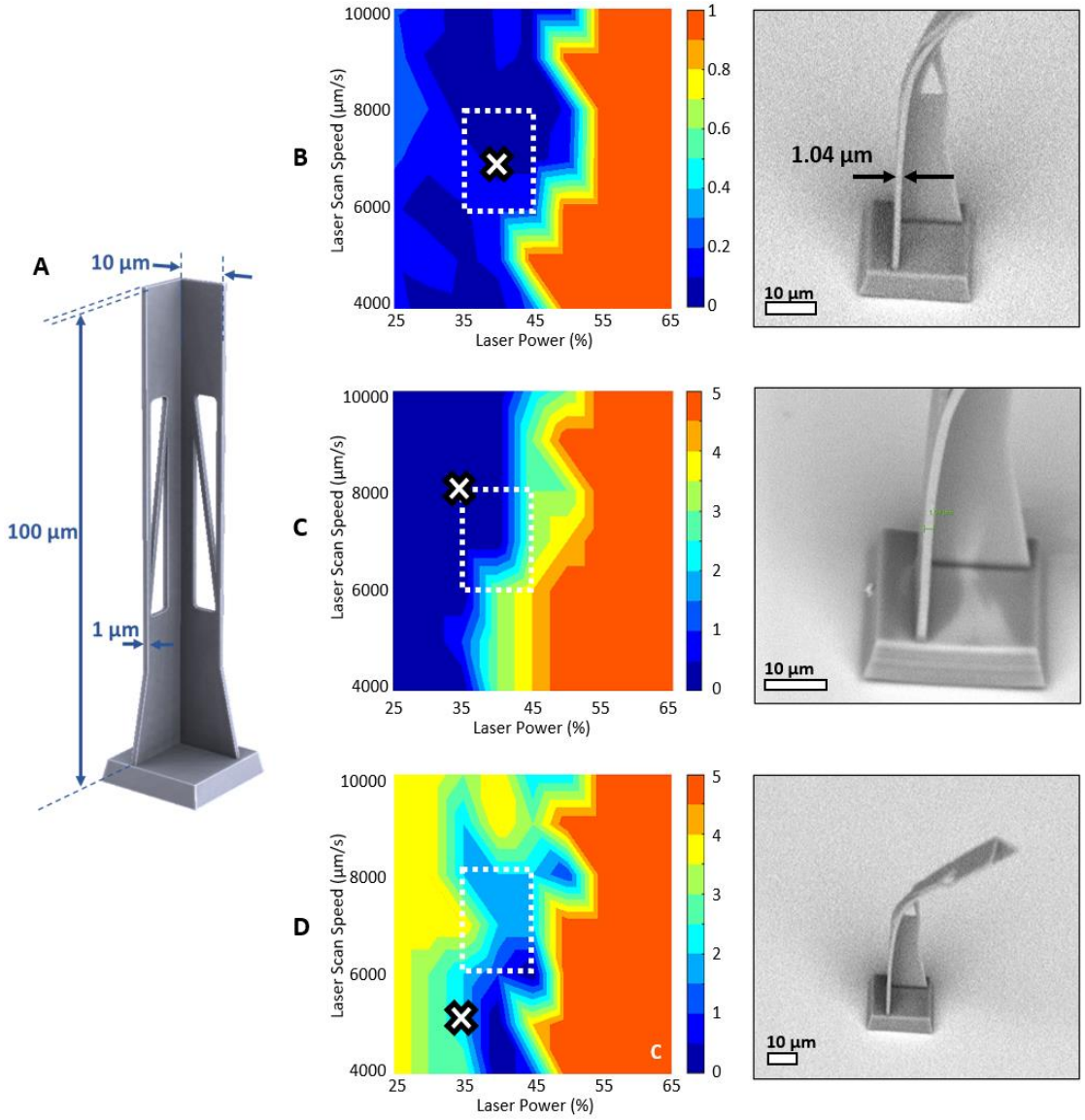

Figure 1. A) CAD model of a 100:1 aspect ratio blade with relevant dimensions. Panel B) shows the deviation from designed dimensions, in µm, where the sample blade (with print settings denoted by an "X" in the contour plot) shows a very small deviation from the 1 µm thickness dimension. Panel C) shows the print defects on a qualitative 0-5 scale (5 is worst), including an SEM image of a blade that has nearly defect-free. Panel D) shows the print distortion on a qualitative 0-5 scale (5 is worst), with the sample SEM image showing a distorted blade which cannot stand in a full vertical position.

conventional tube furnace containing a nitrogen atmosphere at temperatures of 250° C, 400° C, 600° C and 1,000° C, for an hour each. The sample was then allowed to cool down to room temperature at a rate of 5° C per minute. The samples were characterized using a Phenom XL benchtop scanning electron microscope (SEM) in between each step to fully characterize the shrinkage effects of each process.

3. Results

First, the overall print quality of the SiOC structures was explored by both qualitative and quantitative methods before subjecting the structure to the pyrolysis process. First, a tall, thin blade structure with a 100:1 aspect ratio was printed. This L-shaped blade features a height of 100 µm, a width of 10 µm and a thickness of 1 µm, as shown in Figure 1A. Diagonal features were also added to gauge the print quality of non-horizontal and vertical features. These thin, diagonal have a cross section of 1 µm × 1 µm. There are two ways to modulate the power dosage introduced into the resin voxel during printing. Both the laser power and laser scan speed can be tuned for optimal performance. For example, a high dosage would require either a higher laser power setting or a lower laser scan speed. It must be noted that the distance between layers in the z-direction was kept at a constant 500 nm.

The first measure of print quality was the deviation from the designed thickness of 1 µm. Figure 1B shows a contour plot of the thickness deviation for various laser power and laser scan speed settings. This was achieved by printing an array of structures with scan speed intervals of 1,000 µm/s and laser power intervals of 5%. The dotted box within each contour plot represents the area where the print quality is maximized for the polymer-derived ceramic resin. Figure 1B shows that a very small deviation can be initially obtained with a print speed of 7,000 µm/s and a laser power of 40%. The thickness of a blade with these parameters tends to be within the 0.98 µm and 1.03 µm range.

Similarly, prints performed within this power and speed range tend to feature less defects as well. A qualitative scale from 0-5 was generated to judge the level of defects found in the prints.

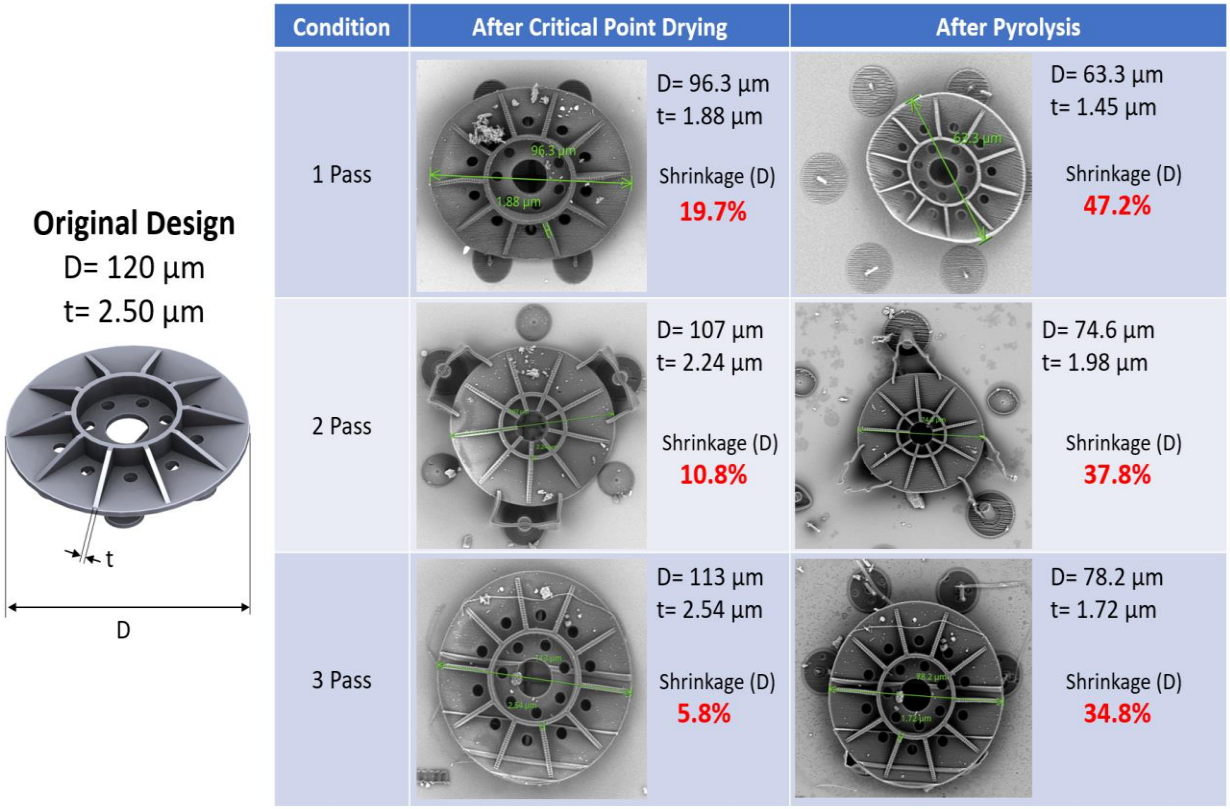

Figure 2. Scanning electron microscope images of a disk microstructure before and after pyrolysis, ranging from n=1,2,3 scans during the 2PP printing process. These disks also feature two separate designs of strain relief legs that are designed to accommodate for the linear shrinkage and maintain the structures in alignment with the center axis before and after pyrolysis

Figure 1C shows an SEM image of a blade printed at 35% laser power and 8,000 µm/s. This blade is relatively free of defects, with only minor blemishes. Some of the defects that do show up include pinholes and small gaps in the bulk material. Most of these defects can be attributed to a high level of energy being introduced into the voxel, essentially "burning" the material. Similarly, if not enough energy is introduced, the material cannot fully cross-link, resulting in gaps and overall shape distortion.

Prints that were not properly energized also displayed high amounts of distortion. For this particular structure, that meant that the blades featured different degrees of curvature and the inability to stand fully upright. Figure 1D shows an SEM image of a blade printed with a speed of 5,000 µm/s and 35% laser power. This blade, though free of visible defects, was not properly cross-linked due to an insufficient power input to the voxels. The blade bent easily during the air-drying process. Blades printed with settings within the dotted box tend to stand upright or have a slight bend to them, especially at lower power and higher scan speed settings.

After gaining an understanding of the optimal print parameters, a disk geometry, like the one showed by the left panel of Figure 2, was created to understand how pyrolysis affects shrinkage in the structure and some potential ways to mitigate it. The disk structure features two separate leg designs that function as strain relief structures, bending inward as the disks isotopically shrink. This is meant to keep the center axis of the disk in the same location during shrinkage. The disks themselves are 120 µm in diameter with a characteristic thickness of 2.5 µm.

Using the lessons learned from the first part of the experiment, the disks were printed at 7,000 µm/s and 40% laser power. One of the key variables that were tested was the number of scanned passes per print. The goal of this experiment was to gauge the effect on shrinkage of the total energy provided to each voxel through a multi-pass approach. For samples that only had a single pass of the scanner, shrinkage was as high as 47.2 %. At this large shrinkage, the strain relief structures failed, as shown in the top-right panel of Figure 2. This shrinkage was reduced to 37.8% when two passes were performed. Lastly, three passes per voxel were also tested, resulting in a shrinkage of 34.8%.

Doing more than three passes did not yield any significant improvements in the amount of shrinkage. The material seems to saturate at three passes and is fully cross linked. The majority of the shrinkage occurs during the pyrolysis process, but surprisingly, the material shrinks a significant amount after critical point drying. This is likely due to some of the un-energized material being extracted from the structure during the process. Though it may help with the reduction in shrinkage, the multi-scan process can produce defects in the print.

In particular, the three-pass prints features line that rise from flat surfaces when they should not, as shown in the 3-pass SEM images in Figure 2. These are due to the fact that once the voxel has been energized, its focus plane slightly changes due to the change in the material. This is commonly referred to as a shadowing effect caused by fully or partially polymerized layers. This effect can result in features being shifted in the z-plane by as much as a 0.25-0.5 µm, based on white light profilometer measurements.

4. Conclusion and Future Work

Ceramic materials bring forth a host of advantages of conventional polymer materials. This will allow devices printed with ceramic resins to operate in more extreme environments where high mechanical properties, low thermal conductivity and electrical insulation may be required. Advances in this field can result in technological leaps in the MEMS/NEMS field. However, the problem of shrinkage must be properly addressed and accounted for before many of these advances can occur. This work lays a groundwork for two separate methods of minimizing and/or accounting for this shrinkage. The first method is using a multi-pass approach to increase the overall dosage and cross-linking of the material before it is dried and pyrolyzed. Second, using strain-relief structures to keep the print centered as it shrinks.

Future work will focus on further developing these two methods to combat shrinkage. Additionally, the transfer of ceramic prints onto other substrates will be studied for actuators, micro-mirrors, and other dynamic applications. This process would involve managing shrinkage of the printed devices, maintaining their center line position and having built-in features that would allow for a repeatable double stamp process.

Acknowledgments

This work was performed under the auspices of the U.S. Department of Energy by Lawrence Livermore National Laboratory under Contract DE-AC52-07NA27344 (LLNL-CONF-823399) and supported by LDRD 19- ERD-018.

References

[1] Saha, et al. “Scalable Submicrometer Additive Manufacturing.” *Science*, **vol. 366**, no. 6461, 2019, pp. 105–109.

[2] Chu, et al. “Centimeter Height 3D-Printing with Femtosecond Laser Two-Photon Polymerization.” *Advanced Materials Technologies*, **vol. 3**, no. 5, 2018, p. 1700396.

[3] Ngo, Kashani, Imbalzano, Nguyen and Hui. “Additive manufacturing (3D printing): A review of materials, methods, applications and challenges.” *Composites Part B: Engineering*, **vol. 143** (2018).

[4] Zheng, Kurselis, El-Tamer, Hinze, Reinhardt, Overmeyer and Chichkov. “Nanofabrication of High-Resolution Periodic Structures with a Gap Size Below 100 nm by Two-Photon Polymerization.” *Nanoscale Res Lett.,* **vol. 14**, 134 (2019).

[5] Ovsianikov et al. “Two Photon Polymerization of Polymer–Ceramic Hybrid Materials for Transdermal Drug Delivery.” *Int. J. Appl. Ceram. Technol*. 2007, **vol. 4**, issue 1, p. 22–29.

[6] Cui, et al. “Additive Manufacturing and Size-Dependent Mechanical Properties of Three-Dimensional Microarchitected, High-Temperature Ceramic Metamaterials.” *Journal of Materials Research*, **vol. 33**, no. 3, 2018, pp. 360–371.

[7] Eckel, et al. “Additive Manufacturing of Polymer-Derived Ceramics.” *Science*, **vol. 351**, no. 6268, 2015, pp. 58–62. *Nanoscale Res Letters,* **vol. 14,** 134 (2019).

[8] Brigo, Schmidt, Gandin, Michieli, Colombo and Brusatin. “3D Nanofabrication of SiOC Ceramic Structures.” *Adv. Sci.* 2018, **vol. 5**, 1800937.

[9] Bauer et al. “Additive Manufacturing of Ductile, Ultrastrong Polymer-Derived Nanoceramics.” *Matter*, **vol. 1**, no. 6, 2019, p. 1547-1556.